Journal of Alloys and Compounds 582 (2014) 364–368

Contents lists available at ScienceDirect

Journal of Alloys and Compounds

journal homepage: www.elsevier.com/locate/jalcom

On relationship between annealing treatment and magnetostriction behavior of Fe–16Cr–2.5Mo damping alloy

Yong-gang Xu *, Xiao-gang Chen

Material Science and Engineering School, Southwest Jiao Tong University, Chengdu 610031, Sichuan Province, PR China

ARTICLE INFO

Article history:
Received 6 May 2013
Received in revised form 6 August 2013
Accepted 8 August 2013
Available online 22 August 2013

Keywords:
Fe–16Cr–2.5Mo alloy
Damping capacity
Annealing treatment
Magnetostriction coefficient

ABSTRACT

The damping capacity of Fe–16Cr–2.5Mo damping alloy was analyzed using a cantilever device. The magnetostriction property was measured using an improved Michelson interferometer. The domain morphology was optically observed using a magneto-fluid. Magnetomechanical Hysteresis Effect (MMHE) was discussed by analyzing the relationship between the magnetostriction performance and the annealing process of the alloy. The results show that the variation of saturate magnetostriction coefficient is quite consistent with that of the damping capacity of the annealed samples. With the local internal stress widely distributing in the annealed alloy, both the domain's mobility and their structure vary with the increasing annealing temperature and time. The local internal stress not only pins the domain mobility but also makes the domain structure disorder. The domain size and the number of 90° magnetic domains are responsible for the highest damping capacity of the sample annealed at 900 °C for 1 h. However, with the prolonged annealing time, the number of 90° domain decreases sharply and more heterogeneous domains appears in the alloy. The spike domains can also pin domain-walls.

1. Introduction

With the development of high-speed transport, vibration and noise are severely deteriorating our civil environment. To solve the problem, much attention is focused on some materials with high damping capacity, especially Fe–Cr damping alloys [1–12]. To date, many believe the magnetomechanical coupling and ΔE effect depend on magnetostriction and anisotropy [13–15], and internal stress is of great importance to the domain's mobility and its structure. In our previous reports [10] on Fe–Cr–Mo damping alloys, it is made clear that larger domain-wall area per unit volume in the alloy causes the alloys to achieve higher damping capacity. The wedge-shaped domains may act as obstacles for pinning the domain walls, lowering the damping capacity of the alloy. Our theoretic calculation [11] shows that smaller domains and sub-domains can dissipate more vibration energy.

Magnetomechanical Hysteresis Effect (MMHE) is the damping mechanism of Fe–Cr alloys, although identifying its role in vibration is very hard. Actually, the magnetostriction coefficient has emerged as a proof of the MMHE in the Fe–Cr damping alloy. Karimi found in Ref. [6] that the variation of the magnetostriction coefficient seems to occur over the same order of magnitude as Q^{-1}. Golovin mentioned that the value of saturation magnetostriction constant depends greatly on a chemical composition and heat treatment of alloys [9]. However, insufficient experimental reports make the identification of the role of MMHE difficult in some cases.

The objective of this paper is to evaluate in detail the effect of annealing treatment on the magnetostriction behavior, and to correlate it with the MMHE of Fe–16Cr–2.5Mo alloy. The relationship among the damping capacity, magnetostriction coefficient, and magnetic domain morphology of the annealed Fe–16Cr–2.5Mo alloy was discussed. It is found that the internal stress was abated through the annealing treatment, increasing the domain mobility and structure. As a result, the damping capacity and MMHE varied with annealing parameters.

2. Experimental procedure

The nominal composition of the alloy was Fe–16Cr–2.5Mo (wt.%). The alloy was melt and cast in a vacuum induction furnace under an argon atmosphere. To completely dissolve atoms in alloy, the cylindrical ingot was solid solution treated at 1150 °C for 10 h. Then the ingot was hot-rolled at approximately 1000 °C for achieving elongation and fragmentation of cast grains. Seven beam samples of the alloy were cut from the hot-rolled ingot by a wire-cut EDM. Their size is $1 \times 10 \times 110$ mm. Then the samples were annealed in vacuum furnace followed by water-quenching. The annealing process is shown in Table 1.

The damping measurement was conducted on a cantilever device according to ASTM standard E756-04. The sample was excited by using a hammer. The vibration response of the sample was measured by an accelerometer. Its frequency–response curve is illustrated in Fig. 1.

The damping value Q^{-1} of the annealed samples is expressed by

$$Q^{-1} = \frac{\Delta f}{\sqrt{3} f_0} \tag{1}$$

* Corresponding author. Tel.: +86 02887600712.
E-mail address: yonggang2002@163.com (Y.-g. Xu).

0925-8388/$ - see front matter © 2013 Elsevier B.V. All rights reserved.
http://dx.doi.org/10.1016/j.jallcom.2013.08.070

Nomenclature

Q^{-1}	internal friction
MMHE	magnetomechanical hysteresis effect
EDM	electrical discharge machining
$\Delta f = f_2 - f_1$	half-power bandwidth, and
f_0	resonance frequency
λ	magnetostriction coefficient
λ_s	saturate magnetostriction coefficient
N	number of lost light circles
λ_0	wavelength of the He–Ne laser, around 632.8 nm
L	net length of the samples

Table 1
Annealing parameters for samples.

No.	Heating temperature (°C)	Heating time (h)
1	800	1
2	900	1
3	1000	1
4	1100	1
5	900	2
6	900	3
7	900	4

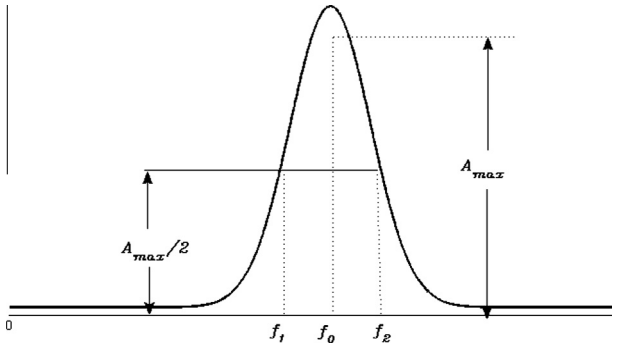

Fig. 1. Resonance curve of a sample.

where Δf, f_2–f_1, represents the half-power bandwidth, and f_0 the resonance frequency for the curve in Fig. 1. Every sample was tested five times, and the mean value represents the damping capacity of the sample.

To measure the magnetostriction value, we designed the gripping heads of an Michelson interferometer for firmly grasping the above-mentioned annealed beam samples. The improved set-up is shown in Fig. 2. In this figure, the magnetic coil around a beam sample produced an tunable axial magnetic field. Thus, the magnetostriction coefficient can be calculated by

$$\lambda = \frac{N\delta}{2L} \tag{2}$$

where N, δ and L represent, respectively, the number of lost interference fringes due to magnetostriction effect, the wavelength of the He–Ne laser light (around 632.8 nm), and the net length of the samples.

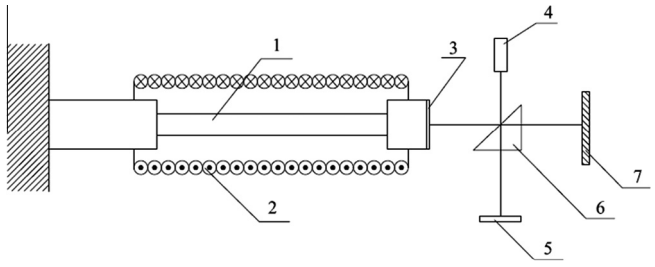

Fig. 2. Improved Michelson interferometer: 1. sample; 2. coil, 3. movable mirror, 4. laser device, 5. firmed mirror, 6. mirror, and 7. screen.

To illustrate the role of annealing treatment on the microstructures of the alloy, several specimens were cut from the annealed samples. After the specimens were mechanically polished, some of the specimens were eroded with picric acid solution for observing their metalphological microstructure under the optical microscope. To observe the domain morphology, the other specimens were eroded with the solution of picric acid, ethanol and hydrochloric acid. The domain structure was observed optically by using a water-based magneto-fluid mentioned in Ref. [12].

3. Results and discussion

3.1. Recrystallization behavior

Annealing the hot-rolled Fe–16Cr–2.5Mo alloy is necessary to achieve a higher damping capacity. Fig. 3 shows the micrographs of the samples annealed respectively at 800 °C, 900 °C, 1000 °C, and 1100 °C for 1 h. It reveals that the recrystallization and recovery transformations take place during the annealing process. Especially, the shape and size of grains depend on the annealing temperature. At 800 °C, the grain size is only less than 100 μm, and some columnar features are still visible. However, the average grain size of the 1100 °C sample reaches several hundred microns.

3.2. Damping capacity

Fig. 4 shows the dependency of damping capacity on annealing temperature. In the figure, the internal friction value is the highest at the annealing temperature of 900 °C. Until now, many researchers attribute the internal friction of the alloy to the MMHE, the result of domain irreversible motion during vibration. It is believed that most internal stress was decreased in the annealing treatment, making the magnetic domains easier to move [14]. Smith and Birchak postulated that energy loss can occur only if the vibration stress exceeds the local stress barrier opposing domain wall motion [12]. Moreover, the amount of dissipated energy also relies on the domain-wall area per unit volume in a grain [10]. Our experimental results demonstrate the above-mentioned performances. The factors contribute to a peak of Q^{-1} with the increase of annealing temperature in Fig. 4. Similarly in Fig. 5, the internal friction reaches the highest at the annealing temperature of 900 °C for 1 h.

3.3. Magnetostriction behavior

Now that the annealing treatment influences the above-mentioned MMHE, we made a particular attempt to measure the magnetostriction coefficient values of the annealed samples. The experimental results are shown in Fig. 6. The annealing process is shown in Table 1. It is worthy of being noted that the highest value of saturate magnetostriction coefficient appears at 900 °C for 1 h, which is quite consistent with that of damping capacity in Figs. 4 and 5. Like the damping performance in Fig. 4, the saturate magnetostriction coefficient of 800 °C is also higher than that of 1000 °C. Considering the argument of Karimi et al. in 2000 [6], we speculate that, by measuring the saturate magnetostriction coefficient, a physical parameter, the role of MMHE in ferromagnetic damping alloys may be understood.

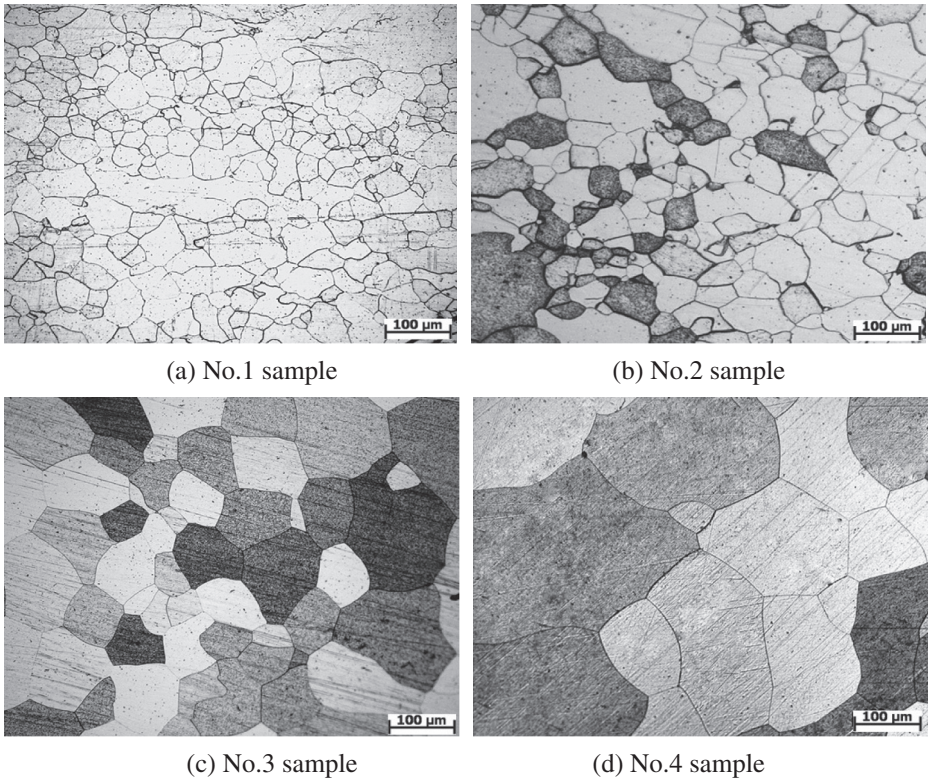

(a) No.1 sample (b) No.2 sample

(c) No.3 sample (d) No.4 sample

Fig. 3. Optical microstructure of Fe–16Cr–2.5Mo samples annealed at different temperatures.

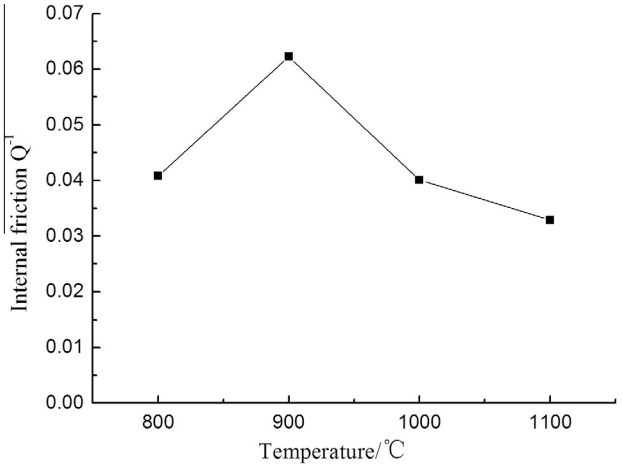

Fig. 4. Damping capacity versus annealing temperature (for 1 h).

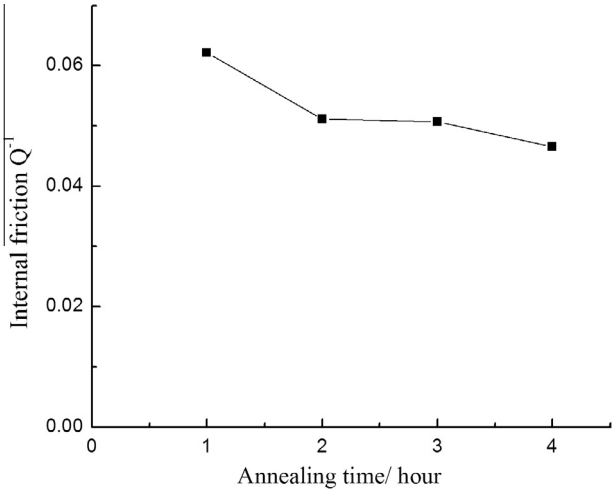

Fig. 5. Damping capacity versus annealing time (at 900 °C).

3.4. Domain morphology

To better understand why the saturate magnetostriction coefficient changes at different annealing treatments, a water-based magneto-fluid was used to observe the magnetic domain morphology under optical microscope. The experimental results are shown in Figs. 7 and 8. In the figures, both the domain's mobility and their structure vary with the increasing annealing temperature and time. Compared to the samples of other annealing temperatures, the domain structure at 800 °C is much more irregular in Fig. 7. It reflects that because the annealing temperature of 800 °C is too low, a large amount of local internal stress distributes in the texture, not only pinning the domain mobility but also making the domain structure disorder. It also shows that as the annealing temperature increases, the domains on the surface of samples are becoming more and more coarser due to the lower local stress. Especially, the number of wedge-shaped domains gradually increase, which were shown in the texture in Fig. 7(d). These domains' characteristics and their negative roles to damping capacity were demonstrated in Refs. [10,11].

We also optically observe the domain morphology of the 900 °C annealed samples. Fig. 8(a) shows their domains. It can be seen that as to the samples annealed for 1 h, the 90° domains is much more, and their size is relatively smaller. Pulino-Sagradi et al. [16] argued that there is a tendency of increasing damping capacity as the volume-fraction of 90° domains increases. However, with

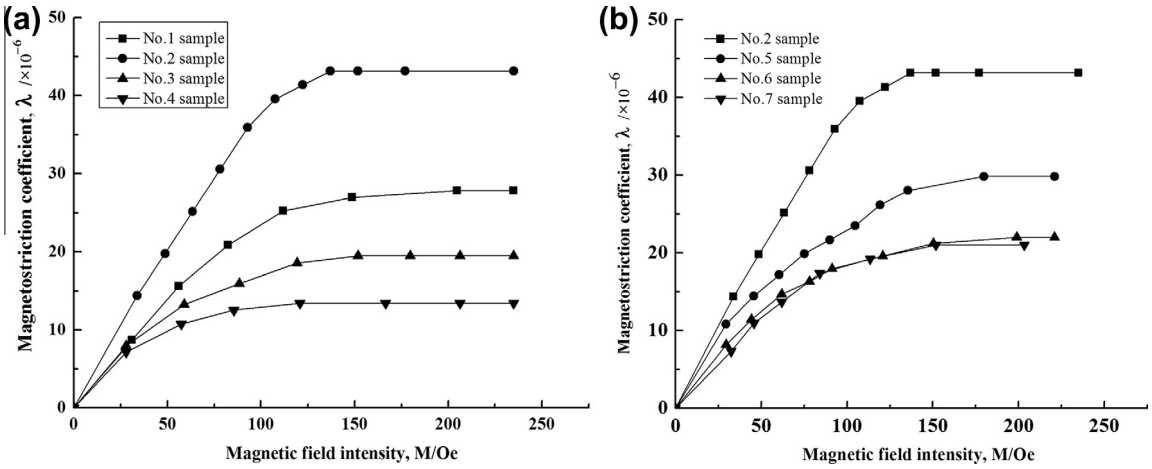

Fig. 6. Magnetostriction coefficient versus annealing temperature for 1 h (a) and annealing time at 900 °C (b).

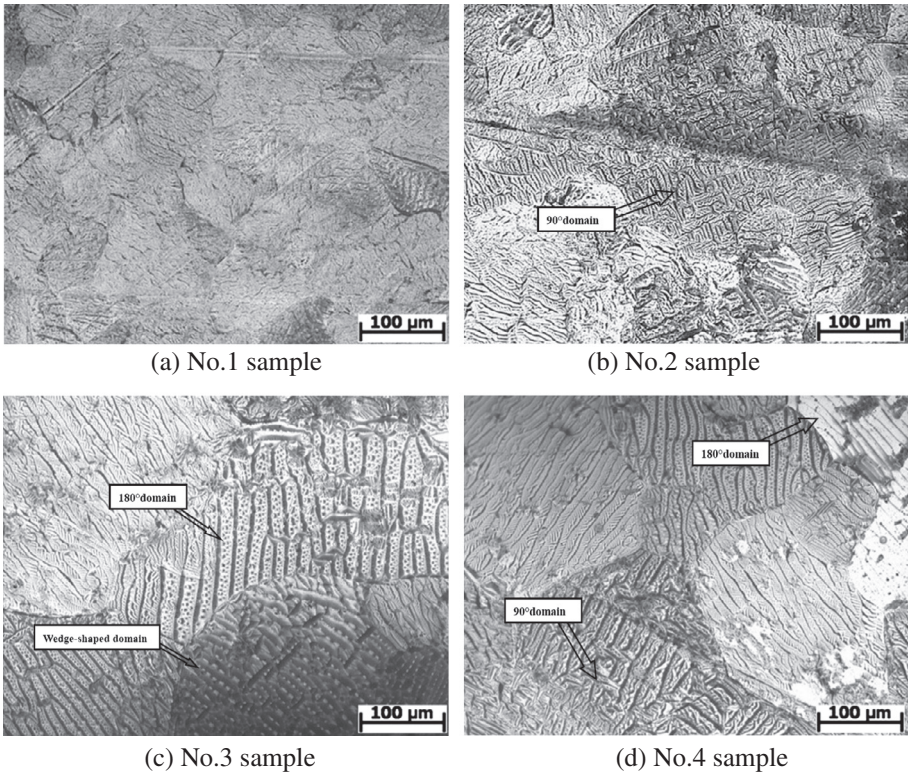

(a) No.1 sample (b) No.2 sample

(c) No.3 sample (d) No.4 sample

Fig. 7. Domain morphology of Fe–16Cr–2.5Mo alloy annealed at different temperatures (for 1 h).

the prolonged annealing time, the number of 90° domains decreases sharply and domains were more heterogeneous in the alloy. Especially, as shown in Fig. 8(d), some spike domains appear in the sample annealed at 900 °C for 4 h. It has been reported in Ref. [17] that this kind of domain can also pin domain-wall, deteriorating the damping capacity of the Fe–Cr alloy. From the point of view, the domain morphology strongly relies on annealing treatment, affecting the role of MMHE in the alloy.

4. Conclusions

The damping mechanism of Fe–Cr based alloy, MMHE, is responsible for the damping capacity variation of the annealed alloys. The experimental results show that the variation of saturate magnetostriction coefficient is quite consistent with that of damping capacity, which suggests that the saturate magnetostriction coefficient may be correlative with the MMHE of ferromagnetic damping alloys. The optical observation results show that with the recrystallization and recovery happening in the texture of the annealed alloy, the local internal stress decreases gradually, promoting the domain walls movable and domain structure varying. The domain size and the number of 90° magnetic domains are responsible for the highest damping capacity of the sample annealed at 900 °C for 1 h. However, with the prolonged annealing time, the number of 90° domain decreases sharply and domains were more heterogeneous in the alloy.

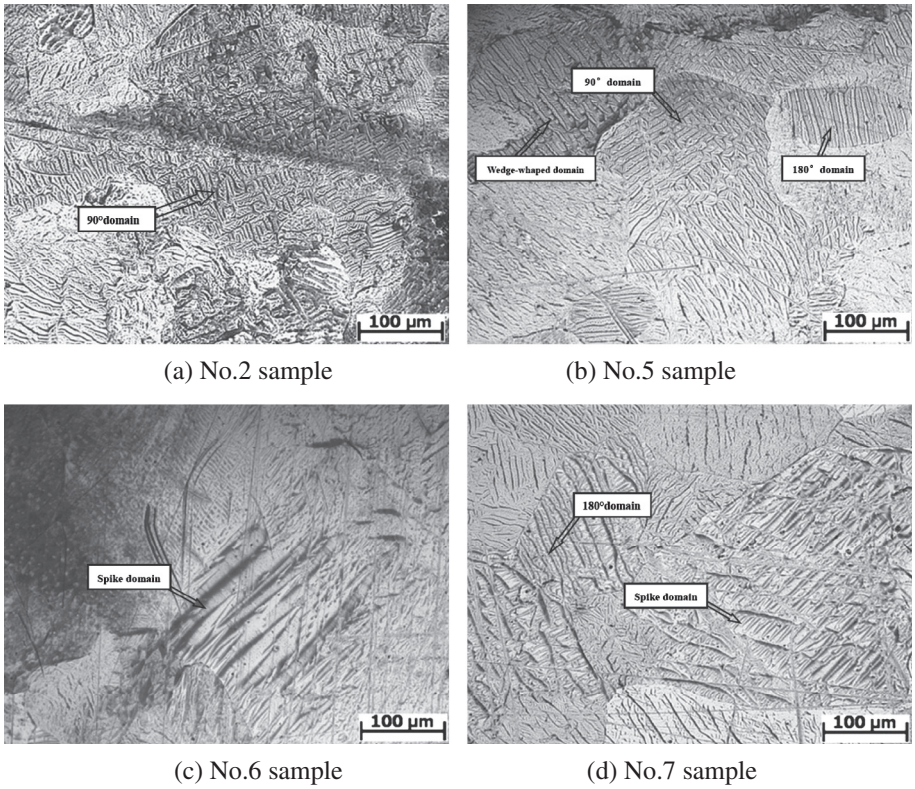

(a) No.2 sample (b) No.5 sample

(c) No.6 sample (d) No.7 sample

Fig. 8. Domain morphology of Fe–16Cr–2.5Mo samples annealed for different hours (at 900 °C).

Acknowledgement

The National Science Foundation of China (NSFC) is acknowledged for financial support of the Project (No. 11172248).

References

[1] G.W. Smith, J.R. Birchak, J. Appl. Phys. 39 (1968) 2311–2315.
[2] Hakaru Masumoto, Showhachi Sawaya, M. Hinai, Trans. JIM 20 (1979) 409–413.
[3] W. Schneider, P. Schrey, G. Hausch, J. Phys. IV (1981). C5-363–C5-369.
[4] L. Xiaodong, W. Baorong, Mater. Sci. Eng. B18 (1993) L1–L3.
[5] I.S. Golovin, Metall. Mater. Trans. A 25A (1994) 111–124.
[6] A. Karimi, Ch. Azcoitia, J. Degauque, J. Magn. Magn. Mater. 215–216 (2000) 601–603.
[7] Weiguo Wang, B. Zhou, Mater. Des. 24 (2003) 163–169.
[8] R. Lin, F. Liu, M. Cao, R. Yang, Acta Metall. Sin. 41 (2005) 958–962.
[9] I.S. Golovin, V.I. Sarrak, S.O. Suvorova, Mater. Sci. Forum 191–121 (1993) 413–418.
[10] X. Yong-gang, L. Ning, W. Yu-hua, J. Magn. Magn. Mater. 323 (2011) 819–821.
[11] Y.-g. Xu, N. Li, Y.-h. Wen, X.-g. Chen, J. Alloys Comp. 539 (2012) 36–39.
[12] G.W. Smith, J.R. Birchak, J. Appl. Phys. 40 (1969) 5174–5180.
[13] Z. Kaczkowski, Mater. Sci. Eng., A 226–228 (1997) 614–625.
[14] A.L. Morales, A.J. Nieto, J.M. Chicharro, P. Pintado, J. Magn. Magn. Mater. 322 (2010) 1952–1961.
[15] B.K. Kardasheva, K. Van Ouytselb, R. De Batistc, J. Alloys Comp. 310 (2000) 169–172.
[16] D. Pulino-Sagradi, M. Sagradi, A. Karimi, J.L. Martin, Scripta Mater. 39 (2) (1998) 131–138.
[17] X.F. Hu, X.Y. Li, B. Zhang, L.J. Rong, Y.Y. Li, Mater. Sci. Eng., B 171 (2010) 40–44.